Manuscript Details

Manuscript number	MICROC_2019_2385
Title	A multi-analytical approach for the characterization of black crusts on the facade of an historical Cathedral
Article type	News
Keywords	Black crusts, marble stone, cultural heritage, conservation, black carbonaceous particles, urban air pollution
Manuscript category	General
Corresponding Author	Valeria Comite
Corresponding Author's Institution	Università degli Studi di Milano
Order of Authors	Valeria Comite, Jose Santiago Pozo-Antonio, Carolina Cardell, Luciana Randazzo, Mauro La Russa, PAOLA FERMO

Submission Files Included in this PDF

File Name [File Type]

Dear Editor.docx [Cover Letter]

Manuscript.docx [Manuscript File]

Fig. 1.tif [Figure]

Fig. 2.tif [Figure]

Fig. 3.tif [Figure]

Fig. 4.tif [Figure]

CAPTION.docx [Figure]

Table1.docx [Table]

Table 2.docx [Table]

Table 3.docx [Table]

Table 4.docx [Table]

Table 5.docx [Table]

Supplementary material.pptx [Supplementary Material]

To view all the submission files, including those not included in the PDF, click on the manuscript title on your EVISE Homepage, then click 'Download zip file'.

Research Data Related to this Submission

There are no linked research data sets for this submission. The following reason is given:
Data will be made available on request

Dear Editor,

This research study is focused on the characterization of black crusts collected from the Dome of Monza located in the homonymous city (N Italy), a hot spot from the point of view of the atmospheric pollution. These samples have been studied for the first time and the work fits into a broader context based on the analysis of black crusts on stone monuments in urban areas affected by high pollution. The aim was to study the black crusts and substrate specimens by a multi-analytical approach including the analysis of the carbonaceous fraction with an innovative methodology, X-ray Diffraction (XRD), FT-IR spectroscopy, Ion Chromatography (IC), Stereomicroscopy (SM), Polarized Light Microscopy (PLM), High Resolution Scanning Electron Microscopy coupled with Energy Dispersive X-ray spectroscopy (HRSEM-EDX) and Laser Ablation Inductively Coupled Plasma Mass Spectrometry (LA-ICP/MS).

This integrated approach has allowed identifying the sources of pollution responsible for the decay of the building carbonatic materials of the Cathedral.

This Cathedral represents an interesting case study for the scientific community since to date the process of black crusts formation on natural stones has not yet been understood in depth.

On behalf of the coauthors
Valeria Comite

A multi-analytical approach for the characterization of black crusts on the facade of an historical Cathedral

Valeria Comite[a], Jose Santiago Pozo-Antonio[b], Carolina Cardell[c], Luciana Randazzo[d], Mauro Francesco La Russa[d], Paola Fermo[a]

[a] *Dipartimento di Chimica, Università degli Studi di Milano, Via Golgi 19, Milan, Italy;* valeria.comite@unimi.it , paola.fermo@unimi.it

[b] *Departamento de Enxeñaría de Recursos Naturais e Medio Ambiente, Escola de Enxeñaría de Minas e Enerxía, University of Vigo, Campus Lagoas-Marcosende s/n, 36310 Vigo, Spain*; ipozo@uvigo.es

[c]*Department of Mineralogy and Petrology, Faculty of Science, University of Granada, Av. Fuentenueva S/N, 18002 Granada, Spain;* cardell@ugr.es

[d]*Dipartimento di Biologia, Ecologia e Scienze della Terra (DiBEST), Università della Calabria, Via Pietro Bucci, 87036 Arcavacata di Rende, CS, Italy;* luciana.randazzo@unical.it , mlarussa@unical.it

Abstract

This study focuses on the characterization of black crusts collected from the Dome of Monza located in the homonymous city (N Italy), a hot spot from the point of view of the atmospheric pollution. Black crusts and substrate specimens were analysed by a multi-analytical approach including X-ray Diffraction (XRD), FT-IR spectroscopy, Ion Chromatography (IC), Stereomicroscopy (SM), Polarized Light Microscopy (PLM), High Resolution Scanning Electron Microscopy coupled with Energy Dispersive X-ray spectroscopy (HRSEM-EDX) and Laser Ablation Inductively Coupled Plasma Mass Spectrometry (LA-ICP/MS). The characterization of the carbon fraction (organic carbon, OC, and elemental carbon, EC) was performed using a new approach based on the use of Carbon Hydrogen Nitrogen (CHN) analysis and Thermogravimetric Analysis (TGA). The integrated approach allowed the identification pollution sources responsible for the black crusts forming process. The precise identification of the main substances responsible for the surface degradation phenomena, in particular those leading to the blackening and disintegration of the carbonate substrates, is essential for the definition of conservative intervention and maintenance strategies, as well as for the development of emission reduction policies on a local scale.

Keywords: Black crusts; marble stone; cultural heritage; conservation; black carbonaceous particles, urban air pollution

1. Introduction

Atmospheric pollution (such as gases and aerosol particulate matter) interacts with stone materials and generates various typologies of decay [1-5]. Among those we can list, for instance, salt crystallization that can lead to physical stress [6-8] or soiling that may evolve to black crusts when in presence of humidity and absence of water washout processes [9-11]. The formation of black crusts is one of the most dangerous phenomenon in architectural heritage [12-14]. Currently, emissions from mobile combustion sources [15-17] are the main agents responsible for air pollution in cities, although a significant decrease is expected in the next years, due to reinforced pollution prevention law and policies. Especially the monuments located in the historic centres of large cities are subjected to typical anthropogenic emissions. Sulphur dioxide, despite its decreasing concentration emitted in the atmosphere, is the main specie responsible for sulphation process that occurs on the stone [18-25]. Up to now, black crusts have been the subject of numerous studies [13,26-28] which highlighted the importance of investigating this topic in order to study physical-chemical decay of stone surfaces [29-34]. Black crusts formation is not only a form of alteration of carbonate stones but also of other types of rock such as granite [25,35-38].

In this work the results obtained from the analysis of black crusts taken from a historical cathedral, Dome of Monza (dating to15th century), placed in a polluted urban centre in the North of Italy, will be discussed. The cathedral is located in the homonymous city placed ca. 20 km NE of Milan. Monza covers an area of 33.09 km^2 and has 123.776 inhabitants and is the third largest city in the Lombardy region (Northern Italy). The city suffers from high pollution produced by the intense vehicular traffic, the high use of domestic heating, as well as the pollution produced by industrial and agricultural activities typical of the Po Valley. In Monza NO_X emissions are due mainly to traffic (69%) but are also due to domestic heating (12%), industries (12%) and incinerators (3%) while anthropogenic VOC emissions are caused by the use of solvents (69%) and by traffic (9%). NH_3 emissions on a regional scale are due to agriculture and breeding activities. The percentage values listed are higher than those recorded for the city of Milan. Moreover, in spite of SO_2 reduction recorded in atmosphere emissions during the last years (for the city of Monza this pollutant is more attributable to industrial activity (82%) (INEMAR, INventario EMissioni Aria, ARPA Lombardia 2014), the presence of SO_2 still dominates the chemical composition of the deposits in urban environments

Black crusts sampled from the Dome façade studied in the present work, have developed on the different marbles used for the monument construction. In order to completely characterize the samples, several analytical techniques were used such as: XRD, FT-IR/ATR, SM, MLP, HRSEM-

EDX, IC; LA-ICP/MS, CHN and TGA. This integrated approach allowed us to gain information about the composition (chemical and mineralogical) and texture of the crusts making it possible to identify the pollution sources causing the stone decay, as well as the variability in BC composition depending both on the exposure conditions of the analysed crust surfaces and their age (older crusts are present on original marbles and crusts of more recent formation have evolved on integration marbles used during the cathedral restoration).

2. Materials and analytical methods

2.1 Dome of Monza

The samples analysed in this work were taken from the facade of the Dome of Monza (Basilica of San Giovanni Battista) located in Monza in the homonym square (Fig. S1 in Supplementary material). The façade, a remarkable example of 15th-century architecture, and divided into three parts, was designed and finished by Matteo da Campione between 1300-1350; it is characterized by alternating dark and white-colored rows of stone blocks. From the 18th to the 20th centuries several and complexes restoration interventions followed that involved some areas of the façade [39]. The dark and white-colored degraded rows were replaced with new ones, all the missing columns of white marble integrated,and the rose window was consolidated. Furthermore, some elements of the three-light windows and the quadrangular compartments on the black background of the rosettes in the central area were restored. In the final phase, a cleaning restoration was performed in the lower central and upper part of the façade. In 2017 the façade was restored once again.

2.2 Sampling

During the last restoration carried out in 2017, 9 samples of black crusts developed on marble stones, were taken from the Dome façade at different heights (Fig. S2) following the indications of the restorers. The samples show variable color, morphology and thickness, depending on the exposure position and on textural features of the underlying substrate.

Two groups of samples were identified, group A and group B (Fig. 2S), according to the information available on restoration interventions in the specific areas from where they were taken:

- group A is formed by samples 1MD, 3MS and 4MS located at ca. 16m high, and taken from the area restored by Conca (original marbles replaced in 1735); therefore, these crusts are about 280 years old, i.e. a pollutants accumulation of about 280 years was present;

-group B is formed by samples taken from a height of ca. 12m, i.e. 5MC, 6MD, 7MD, 8MD and 9MD, and samples 11MD and 12MD taken at ca. 5 m height (lower part of the façade) in areas that

have never been restored (Fig. S2), therefore, these crusts are about 650 years old, i.e. 650 years of accumulation.

A brief sample description accompanied by information regarding sampling point, height and information on eventual previous restorations is summarized in Table 1.

2.3 Analytical methods

2.3.1. Stereomicroscope (SM)

A stereomicroscope (SMZ 1000, Nikon, Japan) equipped for microphotography was used to look at the chromatic and textural features, as well as the conservation state of the BCs and their marble substrates.

2.3.2. Polarized Light Microscopy (PLM)

Mineralogical composition, texture, microstructure and conservation state of the BCs and the marble substrates were studied by Polarized Light Microscopy (PLM) in transmitted and reflected light using a Carl Zeiss Jenapol U instrument (Germany) with a digital camera (Nikon D-7000). To this end samples were prepared as polished thin sections.

2.3.3 X-ray diffraction (XRD)

Mineralogical composition of the BCs was obtained by means of XRD (Siemens D5000) according to the random powder method. In the diffractograms obtained, relative abundance (semi-quantitative estimation) was determined for each mineral phase using the area of highest-intensity diffraction peaks and the intensity ratios established from artificial mixtures of standard minerals [40].

2.3.4 Fourier transform infrared spectroscopy (FT-IR)

Chemical composition of the BCs was characterized using FT-IR spectroscopy (Thermo Nicolet 6700) in Attenuated Total Reflectance (ATR) mode. Functional groups in the absorbance spectra for each sample were identified.

2.3.5 High Resolution Scanning Electron Microscopy coupled with Energy Dispersive X-ray spectroscopy (HRSEM-EDX)

The micro-texture and chemical composition of the BCs and marbles substrates were analyzed using a HRSEM-EDX. The instrument was a Supra 40Vp Carl Zeiss (Germany) furnished with BSE (backscattered electrons) and SE (secondary electrons) detectors (InLens) that deliver chemical and

morphological images respectively, as well as a microanalysis system (Aztec 3) to provide elemental analyses by EDX (X-Max 50 mm detector). Bulk samples and polished thin sections were mounted on Al stubs with double-sided adhesive C tape and carbon coated. Samples were analyzed under high vacuum level. Single-point analyses were acquired at 10 kV (bulk samples) and 20 kV beam energy (thin sections). High-resolution X-ray maps (1024 x 768 pixels, 10 ms dwell time, 2.5 h acquisition, 20 eV/ch resolution, and 43 to 1000 frames) were obtained from selected areas (thin sections) by compiling elemental distribution maps through the use of the *Find Phases* tool implemented in the Aztec 3 EDX. This allowed us to highlight the amount, location and morphology of crystalline/amorphous phases present in the samples.

2.3.6 Ion chromatography (IC)

Ion Chromatography has been employed to quantify the main ions present in the BCs. Three milligrams of powder, withdrawn from the sample surface, were placed in a test tube and treated with 3mL of MilliQ water. The test tubes were put in an ultrasonic bath for 1 h, then the solutions centrifuged and injected for IC analyses by means of an auto-sampler. Measurements of cationic (Na^+, K^+, Ca^{2+}, Mg^{2+} and NH_4^+) and anionic (NO_2^-, NO_3^-, SO_4^{2-}, Cl^-) species were carried out by using an ICS-1000 HPLC system equipped with a conductivity system detector. More details on the analytical procedure are reported elsewhere [28,41-42].

2.3.7 Laser Ablation Inductively Coupled Plasma Mass Spectrometry (LA-ICP-MS)

BCs as well chemical analyses in terms of trace elements were performed by LA-ICP-MS. This method allows to investigate a great number of elements with spot resolutions of about 40–50 μm, also allowing the determination of micrometric compositional variations [43-45]. Analyses were carried out using an Elan DRCe instrument (Perkin Elmer/SCIEX) connected to a New Wave UP213 solid-state Nd-YAG laser probe (213nm). The analytical procedure to characterize the BCs is well-established in varied studies in the literature [27, 46-48].

2.3.8 Carbonaceous fraction analysis

For quantifying the carbonaceous components present in the BCs, CHN analyses were performed by a CHN analyser (CHNS/O Perkin Elmer 2400 Series II Elemental Analyzer using an accessory for the analysis of solids). TG analyses were carried out by a Mettler Toledo TGA/DSC 3+ instrument which allows simultaneous TG and DSC (Differential Scanning Calorimetry) analyses. The analyses were conducted in the range 30°- 800° C, increasing the temperature with a rate of 20° C/minute. The carbonaceous components were estimated in temperature ranges defined by

previously studied standards and using two different atmospheres, i.e. the inert and the oxidant one.

3 Results

3.1 SM, PLM, XRD and FT-IR analysis

The stereomicroscope (SM) study revealed that all BCs samples exhibit intense black color on surface (except 1MD), though their thickness and surface features vary depending on location and height of sampling in the building. For instance, 12MD sample taken at 5m high is made of 3 layers as clearly seen in Fig. S3a in supplementary material (indicated in the red rectangle); the one in contact with the substrate is orange-brown, on top there is a white layer and above a black layer). Some crusts clearly show particles of different color (white, red and grey) on their surface such as 7MD, 1MD and 11MD samples, these two last displaying uneven surface continuity (Fig. S3 b,c,d).

The PLM study confirmed that all crust substrates are marbles, however exhibiting diverse petrographic characteristics in that marbles are of different types. Fig. 1 shows the marked microstructural differences in terms of crystal size, shape and grain boundaries. Note that all marbles are physically degraded presenting varied damage degree. 1MD and 12MD marbles exhibit granoblastic-heteroblastic fabric and mosaic type distribution of polygonal cleavage crystals forming triple junctions at 120º. 1MD displays the largest crystal size ranging from ca. 0.2 to 1.4mm (Fig. 1a), while crystals size range from ca. 0.2 to 0.5mm in 12 MD (Fig. 1b). Fissures and cracks are abundant in both marbles. 4MS marble exhibits heteroblastic fabric. Crystals have sub-angular to rounded shapes and lobate boundaries with sizes ranging from ca. 50μm to 0.3mm (Fig. 1c). Note the intense cracking of the substrate and the calcite crystals from the marble substrate embedded in the gypsum matrix of the BC (Fig. 1d). The highly degraded 7MD marble (Fig. 1e) has a microstructure made of rounded crystals with a bimodal size distribution (<40 μm to 0.3mm). A porfido-granoblastic fabric characterizes 9MS marble, composed of non-equidimensional rounded shaped-grains ranging in size from few microns to 0.4mm (Fig. 1f). Marble is severely degraded as to develop granular disaggregation.

Gypsum ($CaSO_4$. $2H_2O$) was detected by XRD in all BCs samples as the main mineral phase (Table 2). Moreover, quartz (SiO_2) was detected in all BCs in different amounts, except in 4MS. Other minerals were detected in low amounts: i) weddellite ($CaC_2O_4 \cdot 2H_2O$) was identified in 4MS, 5MC and 9MS (mainly in the latter), and ii) calcite ($CaCO_3$) in 11 MD.

FT-IR analysis confirmed the XRD results; gypsum is the main mineral phase in BCs (Fig. 2). The presence of this mineral is confirmed through the bands assigned to 1) OH functional group related

to the hydration state of the mineral and 2) the S-O vibrations. In the first case, the characteristic OH-(H_2O) bands were confirmed by means of the intense doublet at 3520/ 3401 cm^{-1}, a slight shoulder at 3244 cm^{-1}, two weak bands at 2640 and 2510 cm^{-1} and medium intense peaks at 1682/1618 cm^{-1}. Regarding S-O vibration, the sharped band centred at 1102 cm^{-1} assigned to S-O stretching and the lower intense bands at 667, 596 and 460 cm^{-1} corresponding to S-O bending vibration [49-52]. The detection of quartz by XRD is confirmed by FT-IR through a slight shoulder at 1004 cm^{-1}, typically assigned to the asymmetrical stretching vibration of Si–O of quartz [79,53]. With respect to calcium oxalates, note that the discrimination of weddellite and wheellite is made from the peaks assigned to the symmetric O-C-O stretching vibrations at 1317 cm^{-1} and 1324 cm^{-1} for whewellite and weddellite respectively. In addition, the vibration corresponding to H-O-H vibration of lattice water is detected at 1630 cm^{-1} and 781 cm^{-1} for both oxalates and at 669 cm^{-1} and at 603 cm^{-1} for whewellite and weddellite respectively [46,54]. However, confirmation of the presence of calcium oxalate was only possible in some samples due to two difficulties: 1) the coincidence between the oxalate FT-IR bands between 600 and 700 cm^{-1} with those of gypsum (note that gypsum is the main mineral of all the crusts); and 2) the detection in all samples of a broad shoulder-shaped band around 1370-1400 cm^{-1} that frames the 1314 or 1327 cm^{-1} band of the oxalates. Despite these difficulties, XRD results allowed us to identified this oxalate as weddellite. Therefore, identification of oxalates (weddellite) could be evidenced by FT-IR through the disappearance or smoothing of the doublet at 1681-1619 cm^{-1} of gypsum and its transformation into a wide band nearby these wavenumbers, possibly as a result of the contribution of the 1630 cm^{-1} band (intermediate to double) of weddellite. By means of this doublet modification, the presence of wedellite would be confirmed only in 9MS BC where this oxalate was found in a proportion greater than 3% by XRD. On the other hand, the FT-IR spectrum of the 8MD BC is striking, since here in this sample only gypsum and quartz were detected by DRX. However, the band detected at 1321 cm^{-1} could indicate the existence of calcium oxalate together with the bands at 788 cm^{-1} and 596 cm^{-1}. Calcite, present in trace amounts only in 11MD BC, was identified by means of FT-IR through the FT-IR bands at 1419 and 877, and 713 cm^{-1}. In all the BCs samples, a band around 1400-1370 cm^{-1} is detected; in some cases (1MD, 9MS, 3MS, 7MD, 5MC and 11MD), showing considerable high intensity. This band could be assigned to the symmetric CH_3 bending vibrations and, together with those at 711 and 795 cm^{-1} could indicate the existence of organic matter. Also, the band around 1400-1370 cm^{-1} could be assigned to the asymmetric NO_3 stretching vibrations [49]; this band together with those at 870 and 711 cm^{-1} (characteristic of the bending vibration of NO group) would indicate the presence of nitrate salts.

3.2 HRSEM-EDX and LA-ICP-MS analysis

HRSEM-EDX allowed us to obtain detailed information on crusts' morphologies and their interaction with the substrate, as well as information about the chemical composition of the particles present BCs. Only a few representative samples of Group A (1MD and 4MS) and B (7MD, 9MS and 12MD) were analyzed in this study.

LA-ICP-MS analysis allowed us to determine the trace elements (average concentrations in ppm) related to representative BCs samples (Table 3), in particular, the criteria chosen were: different accumulation time of pollutants, height and location of the specimens on the façade of the Dome (right and left).

Results about trace elements suggest concentration especially for some metals such as: As, Ba, Cd, Cu, Fe, Mn, Ni, Pb, Sb, Sn, Sr, V, and Zn, in agreement with the HRSEM-EDX results. In particular obtained data underline that specimens placed at a lower height (12m and 5m) and with a greater period of accumulation of pollutants (650 years) show higher contents of heavy metals. In particular,12 MD BC, located at 5 m from the floor level, shows the highest concentration values.

3.3 Ion Chromatography

Table 4 reveals that all samples show high sulphate concentrations due to the conversion of calcium carbonate of the marble substrate [52,55-26] into gypsum. Furthermore, low concentrations of chlorides, nitritites and nitrates were also detected. Contrary to what observed in previous works [28,34] sodium, potassium and ammonium were not detected. It is worth to notice how average sulphate concentration is slightly lower in group B, i.e. the older crusts (Table 4) indicating that the crusts grouth is not linear with time.

3.4 Carbonaceous fraction analysis (OC and EC)

The analysis of BCs has shown that sulphur is the most abundant element of anthropogenic origin followed by carbon. The in-depth analysis of carbon could suggest possible pollution sources that cause black crusts formation. Total carbon (TC) is composed of OC (Organic Carbon), EC (Elemental Carbon) and CC (Carbonatic Carbon). In this work CC derives mainly from the marble substrate, although deposition of carbonate-rich soil dust is also possible. EC is responsible for the black colour of the crusts; it has a primary origin and is emitted by combustion processes [57-58]. OC is both of primary origin, emitted by traffic or biomass burning [41,59-60], and of secondary origin; in this case it is formed by gaseous precursors such as VOC [57,61-62]. Elemental analysis by CHN allowed the determination of TC within the BCs. Furthermore TGA has been succesfully applied in the past to discriminate OC from EC [63]. The analysis by TGA/DCS allowed to quantify carbonate carbon

percentage (CC%) while elemental carbon percentage (EC%) has been calculated as described in details in La Russa et al., 2017. The organic carbon percentage (OC%) was obtained by difference (OC= TC – (CC+EC). Table 5 shows the obtained results of the carbon fraction for the two groups of BCs A and B.

The values obtained are different from those obtained from samples collected from other monuments previously analyzied [28,34]. In this study, we have observed higher OC values (on average 3.22 for group A and 4.12 for group B) with respect to EC (on average 0.83 for group A and 1.02 for group B), in accordance with what happens in the aerosol particulate matter in Milan where OC is the main constituent of TC [42,62-64].

4 Discussion

Samples cross-sections examined with PLM allowed the evaluation of the crust-substrate interface. Regardless of the marble substrate, crusts sampled from the highest altitude (16m) are made of a single gypsum layer. 1MD BC (thickness ca. 60-130µm) is composed of well-developed needle-like gypsum crystals which also fill the marble fissures and cracks near the surface. As Fig. 1a shows, the borders of crystals near the surface are intensely fractured into micrometric grains. Instead, gypsum crystals in 4MS crust display both prismatic and granular habits yielding a thick crust (thickness ca. 145µm) with copious embedded BCP (Black Carbonaceous Particles) (Fig. 1c,d). BCs are clearly stratified in several layers of different nature, color and thickness in the BCs samples from group B (see Fig. 1s). Here, an orange-brown layer appears at the contact between the substrate and the crust. This layer was identified as weddellite by Capittelli et al. [54]. This layer is called patina noble [65]. At 12m high in the building, 9MS (thickness ca. 100-200µm) and 7MD (thickness ca. 330 µm) BCs exhibit, above the orange-brown layer, a gypsum layer embedding (sub)-spherical BCP in addition to red, yellow and grey particles (Fig. 1g,h). At 5m height, 12MD BC (thickness ca. 270 µm) show the orange-brown layer which is discontinuous since it is fissured and filled by acicular microcrystalline gypsum crystals (Fig. 1b). The surface of the crust shows intense black color due to the abundant spheroidal BCP (Fig. 1b).

SEM images of bulk 1MD and 4MS (belonging to group A) samples show that crusts are made of an interlocked structure of lenticular and/or hexagonal plate-like crystals arranged as rose-like clusters composed of Ca and S, attributed to gypsum. Fig. 3a is a false-color map based on SEM-EDX elemental mapping of 4MS thin section showing the many fissures of the calcite crystals (from the marble substrate) which are filled by microcrystalline gypsum. Note the copious particles of different nature (e.g. Fe, Si, Mg, Al and Pb) inserted into the gypsum crust matrix. Moreover, as revealed by SEM-SE/BSE analyses, crust contains spherical spongy-like carbonaceous particles (Fig. 3b,c),

rounded Fe-rich particles (Fig. 3d,e), Si-rich particles, and cluster of particles where some of the following components were identified, i.e. Pb-chloride, Ca-fosfate, Zn, V, Cr, Co and Br (Fig. 3e, 3f). Analysis of bulk 7MD, 9MS and 12MD samples (group B) by SEM show that crusts have a powdered texture mostly made of granular and (hexagonal) plate-like gypsum crystals as well as tabular crystals in lesser amount Spheroidal spongy and/or smooth BCP as well as metal particles are more abundant than in crusts from group A (1MD and 4MS). Analysis of BCs cross sections reveals the intense crack network developed in the marble area in contact with the crusts, particularly severe in samples of group B. Though cracks do not show parallel orientation to the crust surface, they have the potential for physical disintegration (Fig. 4a,b,c,d), as proved during handling for microscopic analyses. Fig. 4c shows the dissolution patterns in the calcite crystals and the crystallization of gypsum filling the calcite fissures and cracks (Fig. 4b). SEM-EDX study has also revealed the numerous metal particles embedded in the gypsum crust matrix in BCs from group B, their morphology and distribution (Fig. 4). In particular, the X-ray map of a selected area in the 7MD sample (Fig. 4b) proves the presence of gypsum, Si-rich, Fe-rich, P-rich and Pb-K-rich particles, these last preferentially located at the marble crust interface. Pb enriched level in the inner zone of crusts has been reported elsewhere [66], probably due to the affinity of Pb with calcite from the carbonate substrate. The BC having the most complex structure of all studied crusts is 12MD, sampled at the lowest height in the Cathedral (5m altitude). Note in Fig. 4c and 4d the well-defined layered structure and the abundant and varied particles enclosed within the 12MD BC. Gypsum is present in the threefold layered crust (see Fig. S4). The second non-continuous layer, which is the ticker one, is enriched in Mg and Zn. Si-rich, Si/Na-rich and Fe-rich particles are evenly distributed in the two uppermost layers. Minor amount of Pb were detected as compared to 7MD crust (Fig. 4b,d)

XRD and FTIR results allowed to identify that BCs are composed mainly by gypsum as result of the wet or dry deposition of atmospheric sulphur [67] and the subsequent sulphur reaction with the calcium from the marble, regardless of the age (groups A and B). Despite the most important source of sulphur is SO_2 emissions from fossil fuels, also biological activities and construction materials (mortars and concrete) could contribute in the black crust formation [38, 68-72]. In addition, BCs belonging to group B (650 years old) showed higher quantities of calcium oxalates, since 9MS (mainly), 8MD and 5 MC showed weddellite. In samples from the group A (280 years old), only traces of this mineral were found in 4MS. Capittelli et al. [54] also identified a mixture of calcium oxalate (both weddellite and whewellite) and gypsum in yellow-ochre layer on marble of the Milan Cathedral (Italy). As was found in our samples, Capittelli et al. [54] reported the presence of organic matter and calcite in their patinas. As was indicated by other authors [73-74], calcium oxalates can be formed via biological activity of organisms and reactions of organic compounds in rain or aerosols

with the stone. Despite sources of oxalate can be also the application of substances to preserve the rock surfaces [74], in the current research we do not know if conservation products such as consolidants have been used in these surfaces.

All the analysed samples showed low values of ions concentration can be attributed to the diminishing porosity inside the crusts.

Higher values of TC, OC and EC (see Table 5) have been found for group B which is formed by crusts present on original substrates, because of these samples have more years of pollutant accumulation. It has been evidenced a preferential accumulation of OC in almost all BCs samples. OC/EC ratios show values between 4.5-8.2 (four-point-five and eight-point-two) indicating the formation of secondary organic compounds [75]. This result evidences, contrary to what we believed in the past, that vehicular traffic is not the only source of pollution that affects monuments exposed in polluted urban environment. As previously mentioned, organic substances have different origins also coming from VOC that can be embedded in the BC. We should point out that about 50% of the organic fraction present in powder deposits collected from marble surfaces from in Milan [42] is water-soluble and the presence of these substances can be worrying because contributing to accelerate stone decay. The higher values of OC observed for some of our BCs samples can be attributed to the effect of the biologic colonization that can also develop on the crusts; in fact, some studies indicate [76-79] that these processes could create an excess of organic material. In a recent study, the biological colonization present on the façade of the Dome of Monza [80] has been highlighted. For example, in sample 1MD (Fig. S2c), characterized by a higher OC value with respect to the other samples, this phenomenon was clearly visible. It is also interesting to compare EC/TC ratios with the results obtained for other European cities [34,42,75,81-83]. In fact, groups A and B show an average value of EC/TC (0.18 and 0.14 respectively, see Table 3) lower than those observed for the city of Seville (where the same ratio move in the range 0.22- 0.36 indicating a contribution due to traffic emissions) and Milan (0.5-0.9 indicating also in this case a contribution due to traffic emissions). This confirms that BCs collected from Dome of Monza are influenced by organic substances, probably of secondary origin (because of the high OC/EC ratio).

High CC values detected in group B indicate the greater alteration of the marble substrates as compared to group A of the BCs. In fact, SEM analyses have shown in these BCs samples the presence of calcite crystals embedded in the gypsum matrix coming from the degraded marble substrate (see Fig. 3a). Calcite was also detected by HRSEM-EDX, XRD and FT-IR spectroscopy. TGA allowed the calculation of gypsum percentage in the BCs and the results were validated by IC (Fig. S5). It is worth noting that the amount of gypsum present in the BCs is variable (Fig. S5), in agreement with the results obtained with the PLM study. For example, BC of 4MS sample is made

mostly by gypsum, while the BC of 12 MD sample is formed by two well defined layers, being the outermost layer the one made of gypsum. These differences can be caused by different parameters such as the height of sampling, the morphology of the sampled surfaces (vertical or horizontal), the exposure to atmospheric agents and the wash out. In fact, the dynamics that are put in motion during the sulphation process are very complex.

Since black crusts could be considered as a passive sampler of atmospheric pollution, a deeper investigation of the geochemical features was obtained by measuring the average concentrations of trace elements. The concentrations of the main elements measured within some BCs chosen as representative are show in table 4. In general, the results are characterized by a certain variability among BCs samples. Fe, Pb and Zn are the most abundant elements, while As, Ba, Cd, Cu, Mn, Ni, Sb, Sn and V were always present in a lower amount (in terms of average concentrations).

This difference among the analysed BCs samples can be due to several factors such as: different accumulation period, different height of sampling, different exposure to sources of and to wash out.

Sample 12DM shows the highest concentrations of heavy metals, since this sample was taken from the lower part of the façade, most exposed to vehicular traffic and characterized by a longer pollutants accumulation period. On the contrary, samples 1MD and 4MS, show the lower concentration of heavy metals because were taken from the highest areas not directly exposed to vehicular traffic and also affected by a lower accumulation period. Specimens 9MS and 7MD BCs, display intermediate concentrations in heavy metals because taken from a medium height compared to the other samples, but whit a period of accumulation higher then samples 1MD and 4MS.

In general, all samples show high contents of Fe, related to emissions from the numerous industries (oil refining, storage, metal extraction and metallurgy, energy production and distribution, and waste incinerator) placed in the near industrial area of Po valley [84-85]. In addition, the highest concentrations of Pb, Fe, and Zn observed for BCs of group B are in agreement with the use of lead gasoline (15, 86-91Rodriguez-Navarro and Sebastian 1996), employed until about 25 years ago. At the same time, Cu, Ni, Cr, and V well match with the use of other combustibles such as: oil combustible, diesel, and gasoline [15, 86-91], widespread after the abolition of leaded gasoline.

The enrichment observed in group B is mainly due to the high vehicular traffic that characterizes the city of Monza and the metropolitan area of Milan, although the cathedral has been located in a pedestrian zone in the last decades. In fact, in the past years, numerous vehicles have been authorized to circulate both in the vicinity and inside the square where the monument is located (see Fig.S1). On the contrary, group A samples collected from 16m from the ground, often display lower concentrations of the same heavy metals.

5 Conclusions

BC formed on marble stones have been collected from the facade of Duomo of Monza and analysed by several analytical techniques. Two groups of samples were identified, group A and group B, according to the information available on restoration interventions in the specific areas from where they were taken. Petrographic analyses have confirmed that those belonging to group B show a more complex stratigraphy attributable to the greater accumulation time of pollutants compared to BCs of group A which show a simpler morphology. Furthermore, XRD and FT-IR confirm that all BCs are mainly composed of gypsum, with some traces of oxalate and quartz was detected in different amounts for the different groups; weddellite was mainly found in samples belonging to the group B (older samples) The analysis of the main ions present in the BCs has shown low concentrations for these. The HRSEM-EDX analysis showed that samples of group B have accumulated more metal particles, in particular, Pb-rich particles that are particularly mixed with Cl, these located in the interface marble-crust because of the affinity of Pb for calcite. Conversely, the Pb-rich particles are present in the surface in group A although in much less amount. Since group B samples are closer to the bottom of the building the impact of vehicle pollution are evident.

As regards the carbonaceous species (OC and EC), it has been demonstrated that there is a preferential accumulation of organic substances, probably of the secondary origin or biological contamination, can be also accumulate.

Significant and different concentration amounts between group A and B by as regards iron, lead, zinc, copper and vanadium have been highlighted; this represents the fingerprint of the air pollution occurred in the different years of deposition in the analysed BCs. In fact, the city of Monza is affected by pollution from the industrial area, as well as from vehicular traffic. The high concentrations of the different species observed in group B are mainly due to vehicular traffic although the cathedral has been located in a pedestrian zone since a few decades. On the contrary, group A samples, collected from low heights, often display lower concentrations of the same heavy metals because they are less exposed to direct emissions.

In conclusion this study confirms the importance of BCs chemical characterization in order to evaluate the actual risk of degradation to which a monument is submitted when exposed to environmental pollution**.**

Acknowledgments

J. Santiago Pozo-Antonio thanks the Spanish Ministry of Economy and Competitiveness (MINECO) for his "Juan de la Cierva-incorporación" (IJCI-2017-3277) contract.

Paola Fermo and Valeria Comite would like to thanks Ing. Benigno Mörlin Visconti for the precious collaboration and Dr. Francesco Piovani for the help during sampling and for the useful discussion.

C. Cardell thanks the financial support provided by Spanish Research Projects AERIMPACT (CGL2012-30729) and EXPOAIR (P12-FQM-1889), the European Regional Development Fund (ERDF), and the Andalusian Research Group RNM-179. SEM-EDX analyses were performed in the Scientific Instrumentation Centre (CIC) of the University of Granada.

Reference

[1] M. Del Monte, C. Sabbioni, O. Vittori, Airborne carbon particles and marble deterioration, Atmos. Environ. 15 (1981) 645–652. DOI :10.1016/0004-6981(81)90269-9.

[2] P. Brimblecombe, History of urban air pollution, in: J. Finger, O. Herter, F. Palmer (Eds). Urban air pollution—European aspects. Kluver, Dordrecht, 1999, pp.7–20.

[3] P. Brimblecombe, Air pollution and architecture, past, present and future, J. Archit. Conserv. 6 (2000) 30–46. https://doi.org/10.1080/13556207.2000.10785268.

[4] A.V. Turkington, B.J. Smith & W.B. Whalley, Short-term stone surface modification; an example from Venice. Proceedings of the 4th international symposium on the conservation of monuments in the Mediterranean basin. Technical chamber of Greece, Rhodes 1, 1997, pp. 359–372.

[5] G. Zappia, C. Sabbioni, C. Riontino, G. Gobbi, O. Favoni, Exposure tests of building materials in urban atmosphere, Sci. Total. Environ. 224 (1998) 235–244. doi:10.1016/S0048-9697(98)00359-3.

[6] S. A. Ruffolo, M. F. La Russa, M. Ricca, C.M. Belfiore, A. Macchia, V. Comite, A. Pezzino, New insights on the consolidation of salt weathered limestone: the case study of Modica stone, Bull. Eng. Geol. Environ. 76 (2017) 11–20. DOI 10.1007/s10064-015-0782-1.

[7] M. F. La Russa, S. A. Ruffolo, M. A. de Buergo, M. Ricca, C.M. Belfiore, A. Pezzino, G. M. Crisci, The behaviour of consolidated Neapolitan yellow Tuff against salt weathering, Bull. Eng. Geol. Environ. 76 (2017) 115–124. DOI 10.1007/s10064-016-0874-6.

[8] M. Ricca, E. Le Pera, M. Licchelli, A. Macchia, M. Malagodi, L. Randazzo, N. Rovella, S. A. Ruffolo, M. L. Weththimuni, M. F. La Russa The CRATI Project: New Insights on the Consolidation of Salt Weathered Stone and the Case Study of San Domenico Church in Cosenza (South Calabria, Italy), Coatings 9, 330 (2019), 1–15. DOI 10.3390/coatings9050330.

[9] P. Brimblecombe, Environment and architectural stone, in: S. Sigismund, R. Snethlage (Eds.) Stone in architecture, 4th, 461st edn. Springer, Berlin, 2001, pp. 317–346.

[10] N. Ghedini, C. Sabbioni, A. Bonazza, G. Gobbi, Chemical-thermal quantitative methodology for carbon speciation in damage layers on building surfaces. Environ. Sci. Technol. 40 (2006) 939–944. DOI 10.1021/es0501641.

[11] N. Marinoni, M. P. Birelli, C. Rostagno, A. Pavede, The effects of atmospheric multi pollutants on modern concrete, Atmos. Environ. 37 (2003) 4701–4712. DOI 10.1016/j.atmosenv.2003.06.001.

[12] A. Bonazza, C. Sabbioni, N. Ghedini Quantitative data on carbon fractions in interpretation of black crusts and soiling on European built heritage. Atmos. Environ. 39 (2005) 2607–2618. DOI 10.1016/ j. atmosenv.2005.01.040.

[13] C. M. Belfiore, D. Barca, A. Bonazza, V. Comite, M.F. La Russa, A. Pezzino, Application of spectrometric analysis to the identification of pollution sources causing cultural heritage damage. Environ. Sci. Pollut. Res. 20 (2013) 8848–59. DOI 10.1007/s11356-013-1810-y.

[14] O. Farkas, S. Siegesmund, T. Licha, Á. Török, Geochemical and mineralogical composition of black weathering crusts on limestones from seven different European countries, Environ. Earth Sci. 77:211 (2018) DOI: 10.1007/s12665-018-7384-8.

[15] C. Rodriguez-Navarro, E. Sebastian, Role of particulate matter from vehicle exhaust on porous building stone (limestone) sulfation, Sci. Total. Environ. 187 (1996) 79–91. DOI 10.1016/0048-9697 (96)05124-8.

[16] M. D. Geller, L. Ntziachristos, A. Athanasios Mamakos, Z. Zissis Samaras, D. A. Schmitz, J. R. Froines, C. Sioutas, Physicochemical and redox characteristics of particulate matter (PM) emitted from gasoline and diesel passenger cars, Atmos. Environ. 40 (2006) 6988–7004. DOI 10.1016/j.atmosenv.2006.06.018.

[17] D. Contini, A. Gambaro, F. Belosi, S. De Pieri, W. R. L. Cairns, A. Donateo, E. Zanotto, M. Citron, The direct influence of ship traffic on atmospheric PM2.5, PM10 and PAH in Venice. J. Environ. Management 92 (2011) 2119–2129. https://doi.org/10.1016/j.jenvman.2011.01.016.

[18] R. Prikryl, J. Svabodová, K. Zák, D. Hradil, Anthropogenic origin of salt crusts on sandstone sculptures of Prague's Charles Bridge (Czech Republic). Evidence of mineralogy and stable isotope geochemistry, Eur. J. Mineral. 16 (2004) 609–18. DOI: 10.1127/0935-1221/2004/0016-0609.

[19] K. Torfs, R.E. Van Grieken, F. Buzek, Use of stable isotope measurements to evaluate the origin of sulfur in gypsum layers on limestone buildings, Environ. Sci. Pollut. Res. 31 (1997) 2650–5. https://doi.org/10.1021/es970067v.

[20] J. M. Vallet, C. Gosselin, P. Bromblet, P. Rolland, V. Vergés-Belmin, W. Kloppmann, Origin of salts in stone monuments degradation using sulphur and oxygen isotopes: first results of the Bourges Cathedral (France), J. Geochem. Explor. 88 (2006) 358–62. DOI 10.1016/j.gexplo.2005.08.075.

[21] J. Schweigstillová, R. Prikryl, M. Novotná, Isotopic composition of salt efflorescence from the sandstone castellated rocks of the Bohemian Cretaceous Basin (Czech Republic), Environ. Geol. 58 (2009) 217–25. DOI 10.1007/s00254-008-1510-y.

[22] N. Schleicher, C. Recio, Source identification of sulphate forming salts on sandstones from monuments in Salamanca, Spain—a stable isotope approach, Environ. Sci. Pollut. Res. 17 (2010) 770–8. DOI 10.1007/s11356-009-0196-3.

[23] W. Kloppmann, P. Bromblet, J.M. Vallet, V. Vergès-Belmin, O. Rolland, C. Guerrot, Building materials as intrinsic sources of sulphate: a hidden face of salt weathering of historical monuments investigated through multi-isotope tracing (B, O, S), Sci. Total. Environ. 409(9): (2011) 1658–69. DOI 10.1016/j.scitotenv.2011.01.008.

[24] S. Kramar, B. Mirtič, K. Knöller, N. Rogan-Šmuc, Weathering of the black limestone of historical monuments (Ljubljana, Slovenia): oxygen and sulfur isotope composition of sulfate salts. Appl Geochem 26(9–10) (2011) 1632–1638. DOI: 10.1016/j.apgeochem.2011.04.020.

[25] T. Rivas, S. Pozo, M. Paz, Sulphur and oxygen isotope analysis to identify sources of sulphur in gypsum-rich black crusts developed on granites. Sci. Tot. Environ. 482–483 (2014) 137–147. doi: 10.1016/j.scitotenv.2014.02.128.

[26] P. Brimblecombe, C. M. Grossi, Aesthetic thresholds and blackening of stone buildings. Sci. Total Environ. 349 (2005) 175–189. DOI: 10.1016/j.scitotenv.2005.01.009.

[27] D. Barca, V. Comite, C. M. Belfiore, A. Bonazza, M. F. La Russa, S. A. Ruffolo, G. M. Crisci, A. Pezzino, C. Sabbioni, Impact of air pollution in deterioration of carbonate building materials in Italian urban environments, Appl. Geochem. 48 (2014) 122–131. DOI: 10.1016/j.apgeochem.2014.07.002.

[28] M.F. La Russa, P. Fermo, V. Comite, C.M. Belfiore, D. Barca, A. Cerioni, M. De Santis, L.F. Barbagallo, M. Ricca, S. A. Ruffolo, The Oceanus statue of the Fontana di Trevi (Rome): The analysis of black crust as a tool to investigate the urban air pollution and its impact on the stone degradation, Sci. Tot. Environ. 593-594 (2017) 297-309. DOI 10.1016/j.scitotenv.2017.03.185.

[29] D. Barca, C. M. Belfiore, G. M. Crisci, M. F. La Russa, A. Pezzino, S A Ruffolo, Application of laser ablation ICP-MS and traditional techniques to the study of black crusts on building stones: a new methodological approach, Environ. Sci. Pollut. Res. 17 (2010) 1433–47. DOI 10.1007/s11356-010-0329-8.

[30] N. Prieto-Taboada, M. Maguregui, I. Martinez-Arkarazo, M.A. Olazabal, G. Arana, J.M. Madariaga, Spectroscopic evaluation of the environmental impact on black crusted modern mortars in urban–industrial areas, Anal. Bioanal. Chem. 399 (2011) 2949–2959. DOI: 10.1007/s00216-010-4324-1.

[31] N. Schiavon, G. Chiavari, D. Fabbri, Soiling of limestone in an urban environment characterized by heavy vehicular exhaust emissions, Environ. Geol. 46 (2004) 448–455. DOI: 10.1007/s00254-004-1046-8.

[32] H. Morillas, M. Maguregui, C. García-Florentino, J.A. Carrero, J.M. Madariaga, The cauliflower-like black crusts on sandstones: a natural passive sampler to evaluate the surrounding environmental pollution, Environ. Res. 17 (2016) 218–232. DOI 10.1016/j.envres.2016.02.015.

[33] V. Comite, M. Álvarez de Buergo, D. Barca, C.M. Belfiore, A., Bonazza, M.F. La Russa, A. Pezzino, L. Randazzo, S.A. Ruffolo, Damage monitoring on carbonate stones: Field exposure tests contributing t,o pollution impact evaluation in two Italian sites, Constr. Buil. Mat. 152 (2017) 907-922. DOI: 10.1016/j.conbuildmat.2017.07.048.

[34] V. Comite, P. Fermo, The effects of air pollution on cultural heritage: the case study of Santa Maria delle Grazie al Naviglio Grande (Milan), E.P.J. Plus. 133 (12) (2018). 556 DOI: 10.1140/epjp/i2018-12365-6.

[35] J. Sanjurjo-Sánchez, J.R. Vidal Romaní, C. Alves, Comparative analysis of coatings on granitic substrates from urban and natural settings (NW Spain), Geomorphology 138 (2012) 231–242. DOI: 10.1016/j.geomorph.2011.09.008.

[36] J. S. Pozo-Antonioa, M.P. Fiorucci, A. Ramila, A.J. López, T. Rivas, Evaluation of the effectiveness of laser crust removal on granites by means of hyperspectral imaging techniques, App. Surf. Sci. 347 (2015) 832–838.

[37] J. S. Pozo-Antonio, A. Ramil, T. Rivas, A. J. López, M. P. Fiorucci, Effectiveness of chemical, mechanical and laser cleaning methods of sulphated black crusts developed on granite, Const. Build. Mat. 112 (2016) 682–690. http://dx.doi.org/10.1016/j.conbuildmat.2016.02.195.

[38] J. S. Pozo-Antonio, M. F. C. Pereira, C. S. A. Rocha Microscopic characterisation of black crusts on different substrates, Sci. Tot. Environ. 584–585 (2017) 291–306. http://dx.doi.org/10.1016/j.scitotenv.2016.12.080.

[39] R. Cassanelli, Monza anno 1300. La Basilica di S. Giovanni Battista e la sua facciata. Comune di Monza. 1988.

[40] C. R. de Kimpe, Clay and silt analysis, in: M. R. Carter (Eds.), Soil sampling and methods of analysis. Canadian Society of Soil Science, Lewis Publisher; 1993. pp. 719–730.

[41] A. Piazzalunga, V. Bernardoni, P. Fermo, R. Vecchi, Optimisation of analytical procedures for the quantification of ionic and carbonaceous fractions in the atmospheric aerosol and applications to ambient samples. Anal. Bioanal. Chem. 405, (2013) 1123–1132. DOI 10.1007/s00216-012-6433-5.

[42] P. Fermo, R. Gonzalez Turrion, M. Rosa, A. Omegna, A new approach to assess the chemical composition of powder deposits damaging the stone surfaces of historical monuments, Environ. Sci. Pollut. Res. 22 (2015) 6262–6270. DOI 10.1007/s11356-014-3855-y.

[43] B. Gratuze, Obsidian characterization by laser ablation ICPMS and its application to prehistoric trade in the Mediterranean and the Near East: sources and distribution of obsidian within the Aegean and Anatolia, J. Archaeol. Sci. 26 (1999) 869–881. DOI:10.1006/jasc.1999.0459.

[44] E. Vander Putten, F. Dehairs, L. André, W. Baeyens, Quantitative in situ microanalysis of minor and trace elements in biogenic calcite using infrared laser ablation-inductively coupled plasma mass spectrometry: a critical evaluation, Anal. Chim. Acta 378 (1999) 261–272. DOI:10.1016/S0003-2670(98)00613-8.

[45] T. Wyndham, M. McCulloch, S. Fallon, C. Alibert, High resolution coral records of rare earth elements in coastal seawater: biogeochemical cycling and a new environmental proxy. Geochim. Cosmochim. Acta 68 (2004) 2067–2080. DOI: 10.1016/j.gca.2003.11.004.

[46] D. Barca, C. M. Belfiore, G. M. Crisci, M. F. La Russa, A. Pezzino, S. A. Ruffolo, A new methodological approach for the chemical characterization of black crusts on building stones: a case study from the Catania city centre (Sicily, Italy), J. Anal. At. Spectrom. 26 (2011) 1000-1011. DOI 10.1039/C0JA00226G.

[47] M.F. La Russa, C.M. Belfiore, V. Comite, D. Barca, A. Bonazza, S.A. Ruffolo, G.M. Crisci, A. Pezzino, Geochemical study of black crusts as a diagnostic tool in cultural heritage, Appl. Phys. A Mater. Sci. Process. 113 (2013) 1151–1162. DOI: 10.1007/s00339-013-7912-z.

[48] M.F. La Russa, V. Comite, N. Aly, D. Barca, P. Fermo, N. Rovella, F. Antonelli, E. Tesser, M. Aquino, S.A. Ruffolo, Black crusts on Venetian built heritage, investigation on the impact of pollution sources on their composition, Eur. Phys. J. Plus 133: 370 (2018). DOI: 10.1140/epjp/i2018-12230-8.

[49] G. Socrates, Infrared and Raman characteristic group frequencies: Tables and Charts. Chichester: Wiley (Pub.), 2001.

[50] M. D. Lane. Mid-infrared emission spectroscopy of sulfate and sulfate bearing minerals. Am. Miner. 92 (2007) 1-18. DOI: 10.2138/am.2007.2170.

[51] N. Schiavon, Kaolinisation of granite in an urban environment. Environ. Geol. 52 (2007) 399-407. DOI 10.1007/s00254-006-0473-0.

[52] D. Gulotta, M. Bertoldi, S. Bortolotto, P. Fermo, A. Piazzalunga, L. Toniolo, The Angera stone: a challenging conservation issue in the polluted environment of Milan (Italy). Environ. Earth. Sci. 69 (2013) 1085–1094. DOI 10.1007/s12665-012-2165-2.

[53] B. J. Saikia, G. Parthasarathy, Fourier Transform Infrared Spectroscopic Characterization of Kaolinite from Assam and Meghalaya, North eastern India, J. Mod. Phys., 1 (2010) 206-210.

[54] F. Cappitelli, L. Toniolo, A. Sansonetti, Advantages of using microbial technology over traditional chemical technology in removal of black crusts from stone surfaces of historical monuments. Appl. Environ. Microbiol. 73(17) (2007)5671–5675. DOI 10.1128/AEM.00394-07.

[55] P. Fermo, S. Goidanich, V. Comite, L. Toniolo, D. Gulotta, Study and Characterization of Environmental Deposition on Marble and Surrogate Substrates at a Monumental Heritage Site Geosciences 8 (2018) 349–266. DOI 10.3390/geosciences8090349.

[56] V. Sabatini, E. Pargoletti, V. Comite, M. A. Ortenzi, P. Fermo, D. Gulotta, G. Cappelletti, Towards Novel Fluorinated Methacrylic Coatings fo Cultural Heritage: A Combined Polymers and Surfaces Chemistry Study, Polymers 11 (2019) 1190–1207. DOI 10.3390/polym11071190.

[57] D. R. Gentner, G. Isaacman, D. R. Worton, A. W. H. Chan, T. R. Dallmann, L. Davisa, S.Liud, D. A. Day, L. M. Russell, K. R. Wilson, R. Weber, A. Guha, R. A. Harley, A. H. Goldstein, Elucidating secondary organic aerosol from diesel and gasoline vehicles through detailed characterization of organic carbon emissions, Proc. Natl. Acad. Sci. U.S.A. 109 (2012) 18318–18323. DOI 10.1073/pnas.1212272109.

[58] S. Fuzzi, M. O. Andreae, B. J. Hueber, M. Kulmala4, T. C. Bon, M. Boy4, S. J. Doherty, A. Guenther, M. Kanakidou, K. Kawamura, V.-M. Kerminen, U. Lohmann, L. M. Russell, U. Poschl, Critical assessment of the current state of scientific knowledge, terminology, and research needs concerning the role of organic aerosols in the atmosphere, climate, and global change, Atmos. Chem. Phys., 6 (2006)2017–2038. https://doi.org/10.5194/acp-6-2017-2006.

[59] I. Vassura, E. Venturini, S. Marchetti, A. Piazzalunga, E. Bernardi, P. Fermo, F. Passarini, Markers and influence of open biomass burning on atmospheric particulate size and composition during a major bonfire event, Atmos. Environ. 82 (2014) 218–225. DOI: 10.1016/j.atmosenv.2013.10.037.

[60] K.R. Daellenbach, C. Bozzetti, A. Křepelová, F. Canonaco, R. Wolf, P. Zotter, P. Fermo, M. Crippa, J.G. Slowik, Y. Sosedova, Y. Zhang, R.-J. Huang, L. Poulain, S. Szidat, U. Baltensperger, I. El Haddad, A. S. H.

Prévôt, Characterization and source apportionment of organic aerosol using offline aerosol mass spectrometry, Atmos. Meas. Tech. 9 (1) (2016) 23–39. https://doi.org/10.5194/amt-9-23-2016.

[61] A. L. Robinson, N. M. Donahue, M. K. Shrivastava, E. A. Weitkamp, A. M. Sage, A. P. Grieshop, T. E. Lane, J. R. Pierce, S. N. Pandis, Rethinking Organic Aerosols: Semivolatile Emissions and Photochemical Aging, Science 315 (2007) 1259 –1262. DOI: 10.1126/science.1133061.

[62] V. Bernardoni, R. Vecchi, G. Valli, A. Piazzalunga, P. Fermo PM10 source apportionment in Milan (Italy) using time-resolved data, Sci. Tot. Environ. 409 (2011) 4788–4795. DOI 10.1016/j.scitotenv.2011.07.048.

[63] P. Fermo, A. Piazzalunga, R. Vecchi, G. Valli, M. Ceriani, A TGA/FT-IR study for measuring OC and EC in aerosol samples, Atmos Chem Phys, 6 (1) (2006) 255–266.

[64] R. Vecchi, V. Bernardoni, P. Fermo, F. Lucarelli, F. Mazzei, S. Nava, P. Prati, A. Piazzalunga, G. Valli, 4-hours resolution data to study PM10 in a "hot spot" area in Europe, Environ. Monit. Assess. 154 (2009) 283–300. DOI 10.1007/s10661-008-0396-1.

[65] R. Rossi Manaresi, Oxalate patinas and conservation treatments, p. 113–127, in: M. Realini and L. Toniolo (Eds.), The oxalate films in the conservation of works of art. Proceedings of the 2nd International Symposium, 25 to 27 March 1996 EDITEAM. Bologna, Italy, 1996, pp. 113–127.

[66] S.A. Ruffolo, V. Comite, M.F. La Russa, C.M. Belfiore, D. Barca, A. Bonazza, G.M. Crisci, A. Pezzino, C. Sabbioni, Analysis of black crusts from the Seville Cathedral: a challenge to deepen understanding the relationship among microstructure, micro chemical features and pollution sources. Sci. Total Environ. 502 (2015) 157–166. DOI 10.1016/j.scitotenv.2014.09.023.

[67] A.E. Charola, R. Ware, Acid deposition and the deterioration of stone: a brief review of a broad topic, Geol. Soc. Spec. Pub. 205 (2002)393–406. https://doi.org/10.1144/GSL.SP.2002.205.01.28.

[68] T. Hosono, E. Uchida, C. Suda, A. Ueno, T. Nakagawa. Salt weathering of sandstone at the Angkor monuments, Cambodia: identification of the origins of salts using sulphur and strontium isotopes, J. Archaeol. Sci. 33: (2006)1541–51. DOI: 10.2465/ganko.93.411.

[69] N. Schleicher, C. Recio, Source identification of sulphate forming salts on sandstones from monuments in Salamanca, Spain—a stable isotope approach, Environ. Sci. Pollut. Res. 17 (2010) 770–8. DOI: 10.1007/s11356-009-0196-3.

[70] W. Kloppmann, P. Bromblet, J.M. Vallet, V. Vergès-Belmin, O. Rolland, C. Guerrot, Building materials as intrinsic sources of sulphate: a hidden face of salt weathering of historical monuments investigated through multi-isotope tracing (B, O, S), Sci. Total. Environ.;409(9) (2011) 1658–69. DOI: 10.1016/j.scitotenv.2011.01.008.

[71] S. Kramar, B. Mirtič, K. Knöller, N. Rogan-Šmuc, Weathering of the black limestone of historical monuments (Ljubljana, Slovenia): oxygen and sulfur isotope composition of sulfate salts, Appl. Geochem. 26(9–10) (2011)1632–8. https://doi.org/10.1016/j.apgeochem.2011.04.020.

[72] J.S. Pozo-Antonio, M.F.C. Pereira, C.S.A. Rocha, I. Puente, C. Figueiredo, Comparative study of deterioration forms on nearby granitic bridges from an urban setting in the NW Iberian Peninsula Geomorphology, 274 (2016) 11-30. https://doi.org/10.1016/j.geomorph.2016.09.009.

[73] M. Del Monte, C. Sabbioni, G. Zappia, The origin of calcium oxalates on histor- ical buildings, monuments and natural out- crops, Sci. Tot. Environ. 67 (1987) 17-39. https://doi.org/10.1016/0048-9697(87)90063-5.

[74] J. Russ, W.D. Kaluarachchi, L. Drummond, H.G.M. Edwards. 1999. The Nature of a Whewellite-Rich Rock Crust Associated with Pictographs in Southwestern Texas. J. Stud. Conserv. 44, Issue 2 (1999) 91-103. https://doi.org/10.1179/sic.1999.44.2.91.

[75] R. Vecchi, M. Chiari, A. D'Alessandro, P. Fermo, F. Lucarelli, F. Mazzei, S. Nava, A. Piazzalunga, P. Prati, F. Silvani, G. Valli, A mass closure and PMF source apportionment study on the sub-micron sized aerosol fraction at urban sites in Italy. Atmos. Environ. 42 (2008) 2240–2253. DOI 10.1016/j.atmosenv.2007.11.039.

[76] D. Camuffo, M. Del Monte, C. Sabbioni, Influenza delle precipitazioni e della condensazione sul degrado superficiale dei monumenti in marmo e calcare. Materiali Lapidei. Volume Speciale del Bollettino, Roma, p.15-36, 1987.

[77] C. Sabbioni, G. Zappia, Oxalate patinas on ancient monument: the biological hypothesis. Aerobiologia Issue 7 (1991) 31–37. doi:10.1007/BF02450015.

[78] C. Sabbioni, Contribution of atmospheric deposition to the formation of damage layers. Sci. Total. Environ. 167 (1995) 49–55. https://doi.org/10.1016/0048-9697(95)04568.

[79] A. Bonazza, P. Brimblecombe, C. M. Grossi, C. Sabbioni, Carbon in black crust from the tower of London. Environ. Sci. Technol. 41 (2007) 4199–4204. https://doi.org/10.1021/es062417w.

[80] D. Gulotta, F. Villa, F. Cappitelli, L. Toniolo, Biofilm colonization of metamorphic lithotypes of a renaissance cathedral exposed to urban atmosphere, Sci. Tot. Environ. 639 (2018) 1480–1490. https://doi.org/10.1016/j.scitotenv.2018.05.277.

[81] C. Saiz-Jimenez, Air pollution and Cultural Heritage. Proceedings of the International, Workshop on Air Pollution and Cultural Heritage, Seville, Spain, 2003.

[82] C. Perrino, S. Canepari, M. Catrambone, S. Dalla Torre, E. Rantica, T. Sargolini, Influence of natural events on the concentration and composition of atmospheric particulate matter, Atmos. Environ. 43 (2009) 4766–4779. DOI: 10.1016/j.atmosenv.2008.06.035.

[83] S. Sandrini, S. Fuzzi, A. Piazzalunga, P. Prati, P. Bonasoni, F. Cavalli, M.C. Bove, M. Calvello, D. Cappelletti, C. Colombi, D. Contini, G. De Gennaro, A. Di Gilio, P. Fermo, L. Ferrero, V. Gianelle, M. Giugliano, P. Ielpo, G. Lonati, A. Marinoni, D. Massabò, U. Molteni, B. Moroni, G. Pavese, C. Perrino, M. G. Perrone, M. R. Perrone, Spatial and seasonal variability of carbonaceous aerosol across Italy, Atmos. Environ. 99 (2014) 587–598. DOI 10.1016/j.atmosenv.2014.10.032.

[84] C. Colombi, Relazione Campagna PoAIR febbraio 2014. Available online: http://www.arpalombardia.it/qariafiles/varie/Relazione%20campagna%20PoAIR%20febbraio%202014.pdf (accessed on 5 August 2019).

[85] EEA Report No 1/2017. Climate change, impacts and vulnerability in Europe 2016 An indicator-based report. European Environment Agency. Luxembourg: Publications Office of the European Union, 2017.

[86] M. D. Geller, L. Ntziachristos, A. Athanasios Mamakos, Z. Zissis Samaras, D. A. Schmitz, J. R. Froines, C. Sioutas Physicochemical and redox characteristics of particulate matter (PM) emitted from gasoline and diesel passenger cars. Atmos Environ 40 (2006) 6988–7004. DOI 10.1016/j.atmosenv.2006.06.018.

[87] J. Sternbeck, A. Sjödin, K. Andréasson, Metal emissions from road traffic and the influence of resuspension results from two tunnel studies, Atmos. Environ. 36 (2002) 4735–4744. DOI 10.1016/S1352-2310(02)00561-7.

[88] D.R. Gómez, M.F. Ginè, A. C. Sánchez Bellato, P. Smichowski, Antimony: a traffic related in the atmosphere of Buenos Aires, Argentina, J. Environ. Monit. 7 (2005) 1162–1168. DOI 10.1039/b508609d.

[89] G. Dongarrà, E. Manno, D. Varrica, Possible markers of traffic-related emissions, Environ. Monit. Assess. 154 (2009) 117–125. DOI 10.1007/s002549900071.

[91] H. Harmens, D.A. Norris, G.R. Koerber, A. Buse, E. Steinnes, A. Rühling, Temporal trends in the concentration of arsenic, chromium, copper, iron, nickel, vanadium and zinc in mosses across Europe between 1990 and 2000. Atmos. Environ. 31 (2007) 6673–6687. DOI 10.1016/j.atmosenv.2007.03.062.

[91] H. Harmens, D.A. Norris, the participants of the moss survey, Spatial and temporal trends in heavy metal accumulation in mosses in Europe (1990–2005). Programme Coordination Centre for the ICP Vegetation, Centre for Ecology & Hydrology. Bangor, UK, Natural Environment Research Council, 2008.

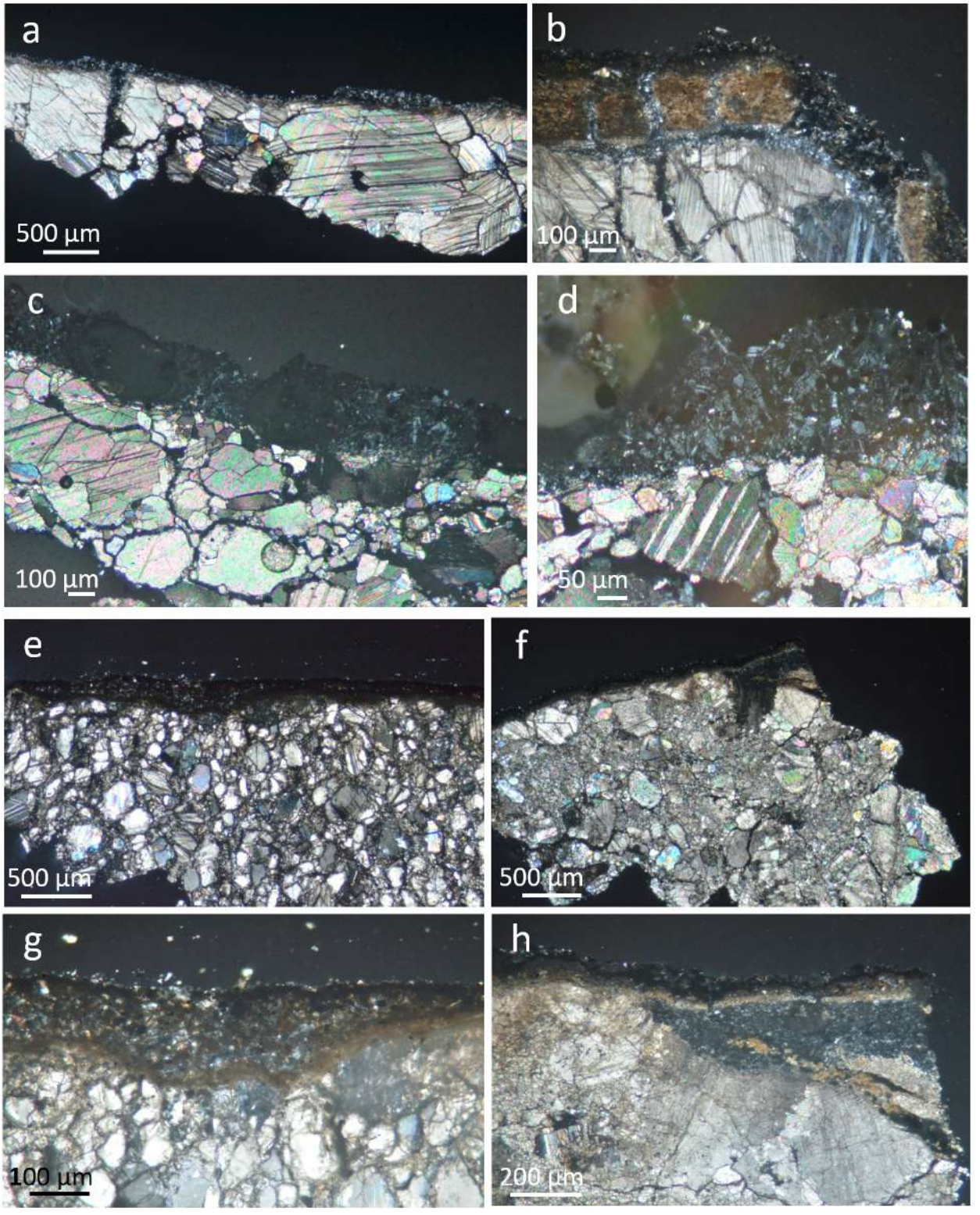
a
500 µm
b
100 µm
c
100 µm
d
50 µm
e
500 µm
f
500 µm
g
100 µm
h
200 µm

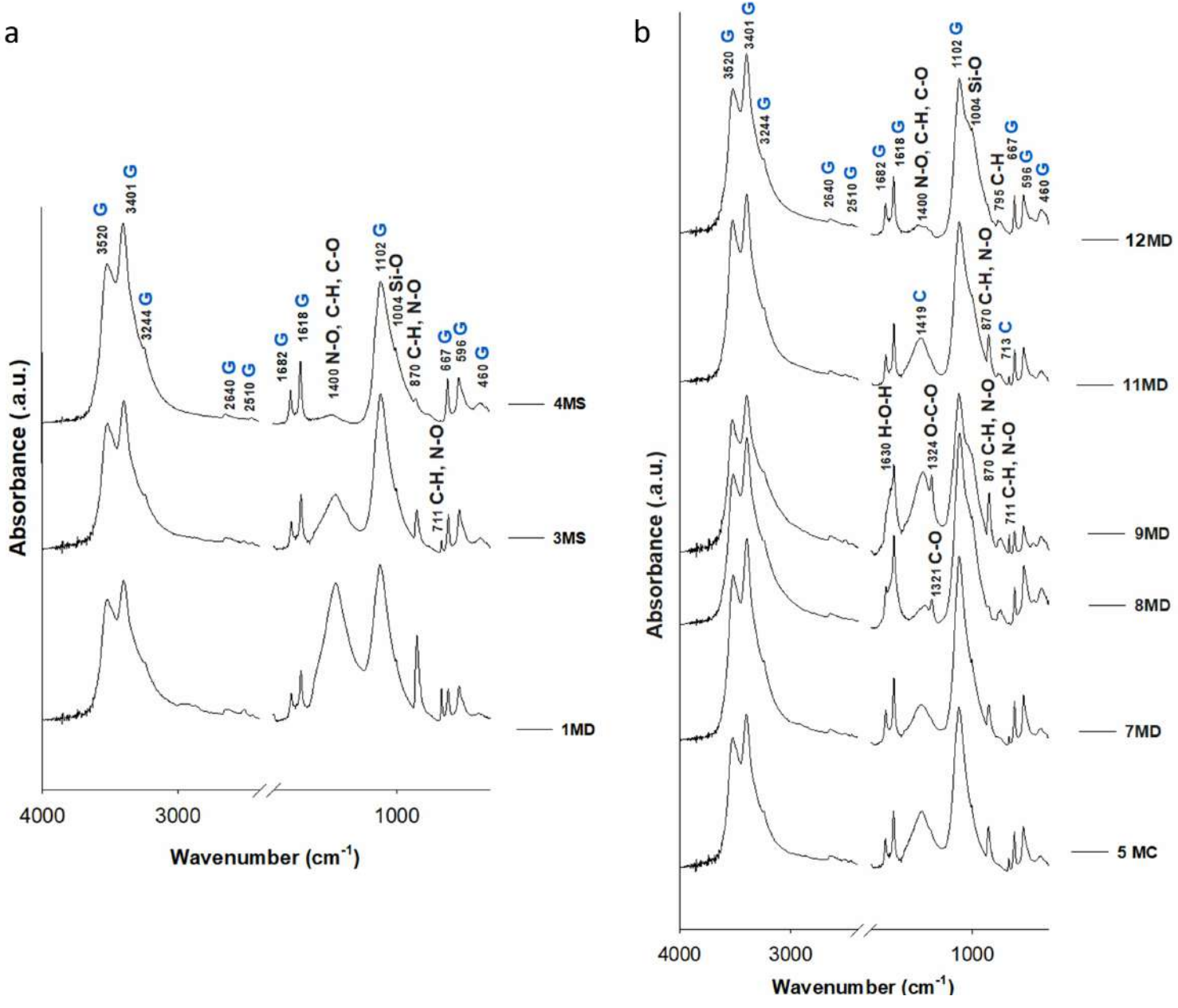
a
Absorbance (.a.u.)
3520 G
3401 G
3244 G
2640 G
2510 G
1682 G
1618 G
1400 N-O, C-H, C-O
1102 G
1004 Si-O
870 C-H, N-O
711 C-H, N-O
667 G
596 G
460 G
4MS
3MS
1MD
4000
3000
1000
Wavenumber (cm-1)
b
Absorbance (.a.u.)
3520 G
3401 G
3244 G
2640 G
2510 G
1682 G
1618 G
1400 N-O, C-H, C-O
1102 G
1004 Si-O
795 C-H
667 G
596 G
460 G
1630 H-O-H
1419 C
1324 O-C-O
1321 C-O
870 C-H, N-O
713 C
711 C-H, N-O
12MD
11MD
9MD
8MD
7MD
5 MC
4000
3000
1000
Wavenumber (cm-1)

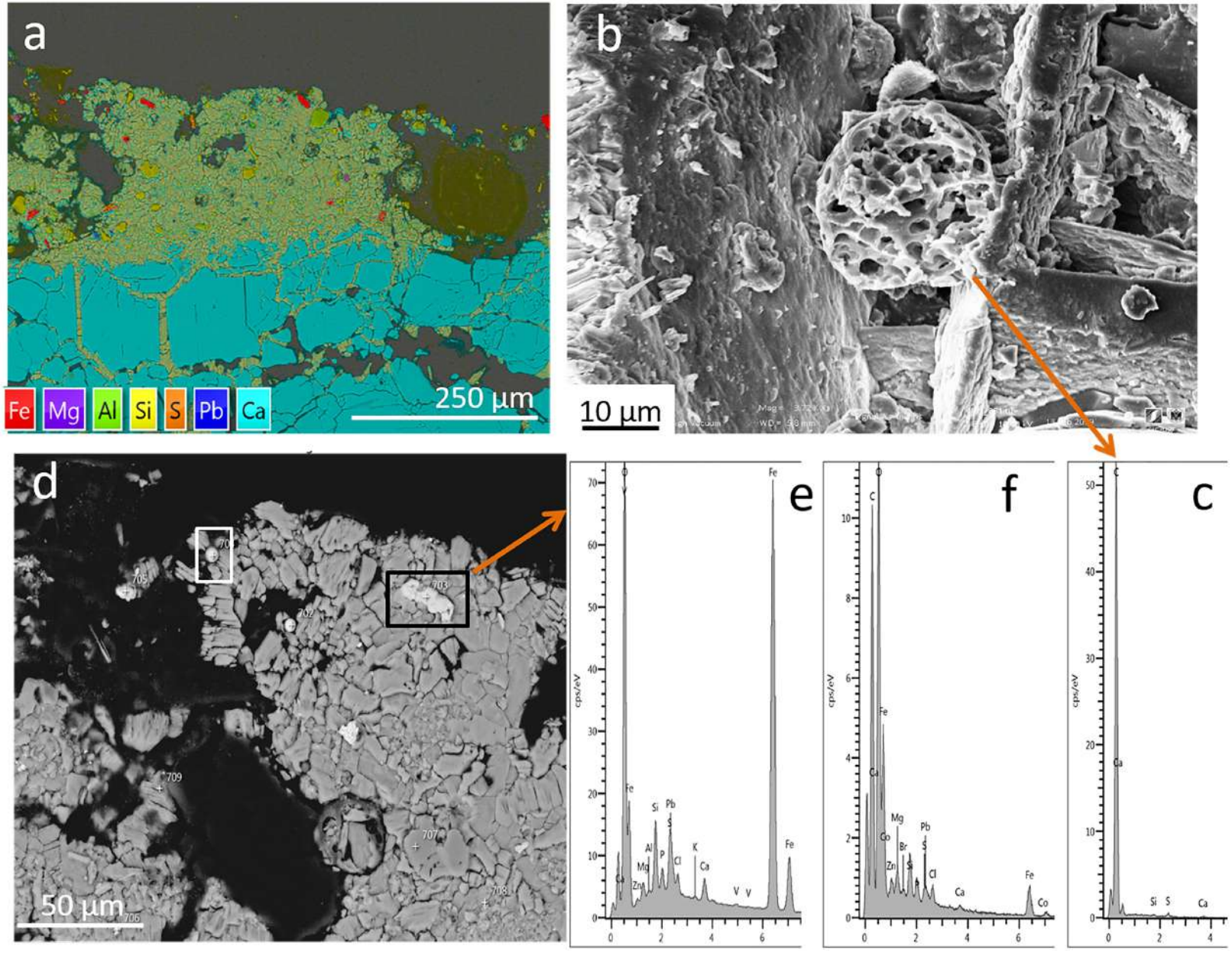
a
Fe
Mg
Al
Si
S
Pb
Ca
250 µm
b
10 µm
d
50 µm
e
f
c
cps/eV

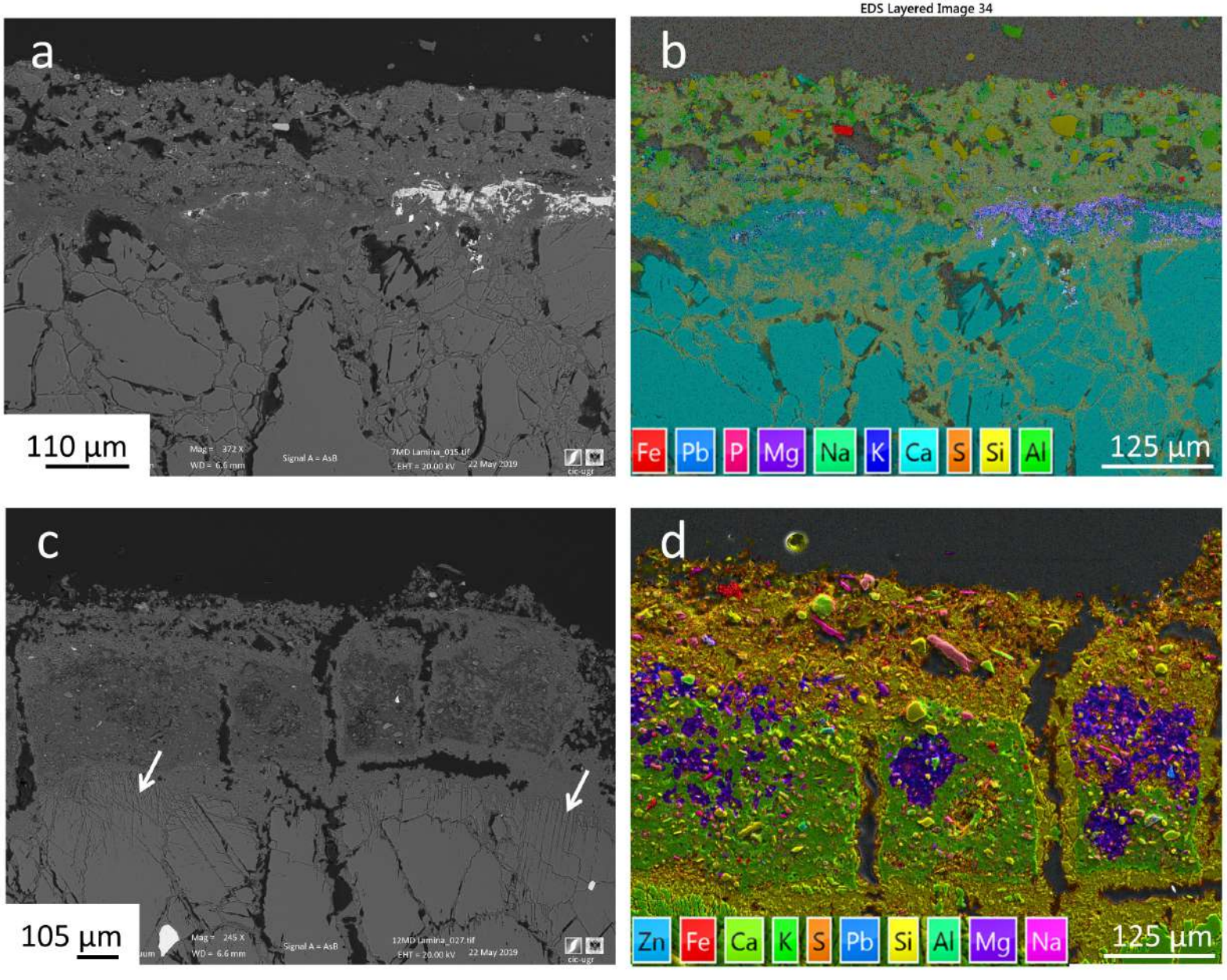
a
110 µm
Mag = 372 X
WD = 6.6 mm
Signal A = AsB
7MD Lamina_015.tif
EHT = 20.00 kV
22 May 2019
cic-ugr
EDS Layered Image 34
b
Fe
Pb
P
Mg
Na
K
Ca
S
Si
Al
125 µm
c
105 µm
Mag = 245 X
WD = 6.6 mm
Signal A = AsB
12MD Lamina_027.tif
EHT = 20.00 kV
22 May 2019
cic-ugr
d
Zn
Fe
Ca
K
S
Pb
Si
Al
Mg
Na
125 µm

Fig. 1 Microphotographs of BCs samples (thin sections) from Monza Cathedral taken with PLM (crossed polars). a) 1MD (16m high), note the large crystal size and the gypsum crystals filling the calcite crystals fissures (arrow); b) 12MD (5m high), note the intense fissure system of the marble, the 3 layers of the crust and the abundant BCPs (arrow); c and d) 4MS (16m high), note the heteroblastic fabric of the marble and the small calcite crystals fragments being incorporated into the gypsum crust (arrow); e) 7MD and f) 9MS (12m high), note the dissimilar marble substrates highly fractured; g) 7MD and h) 9MS, note the orange-brown layer in contact with the marble.

Fig. 2 ATR-FT-IR spectra of the black crusts sampled in Monza Cathedral. a) samples belonging to group A. b) samples belonging to group B. Effects assigned to the absorbance bands are depicted and the minerals detected by XRD are shown in blue (G: gypsum, C: calcite).

Fig. 3. SEM images showing the BC of 4MD sample: a) SEM-EDX false-color mineral map (thin section); note the significant fissure system of the marble -filled by gypsum- originating granular disaggregation, and the particles of varied nature enclosed into the BC, such as Fe-, Pb-, Si-, and Ca-rich particles; b) spherical spongy-like carbonaceous particle; c) EDX spectrum of carbonaceous particle shown in b); d) BSE-SEM image showing rounded Fe-rich particles (white box) and cluster of metal particles (black box); e) EDX spectrum of white box shown in d; f) average EDX spectrum of the black box shown in d).

Fig. 4. SEM microphotographs of 7MD and 12MD BCs (thin sections): a) BSE-SEM image of 7MD showing in brighter grey color the copious metal particles; note their accumulation in the interface between the marble and the BC; b) SEM-EDX false-color mineral map of 7MD; note the high amount of Pb and K in the interface marble-crust; c) BSE-SEM image of 12MD revealing the calcite crystals dissolution patterns (arrows) and the structure of the crust which is detaching from the substrate; d) SEM-EDX false-color mineral map of 12MD clearly showing the composition, morphology and distribution of the particles enclosed in the BC.

Table 1 List of samples collected from the façade of the Dome of Monza.

Sample	Height and location	Description	Stone	Years of Pollutants accumulation
1MD	16 m rose window right side of the façade	Black crust on marble	The stone is a later integration (1735 year)	About 280
3MS	16 m rose window left side of the façade	Black crust on marble	The stone is a later integration (1735 year)	
4MS	16 m rose window left side of the façade	Black crust on marble	The stone is a later integration (1735 year)	
5MC	12 m rose window central part of the façade	Black crust on marble	Original	About 650
7MD	12 m rose window right side of the façade	Black crust on marble.	Original	
8MD	12 m rose window right side of the façade	Black crust and marble	Original	
9MS	12 m left double-arched window, original capital of the façade	Black crust on original marble	Original	
11MD	5 m double-arched window, right side of the façade	Black crust on original marble	Original	
12MD	5 m double-arched window, right side of the façade	Black crust and original	original	

Table 2 Mineralogical composition of the crusts collected in Monza Cathedral. G: gypsum; Q: quartz; C: calcite; WD: weddellite; WW: whewellite. + + + +: > 50%; + + +: 30-50%; + +: 10-30%; +: 3-10%; tr: < 3%. -: not detected.

Samples	G	Q	C	WD	WW
1MD	++++	+	-	-	-
3MS	++++	+	-	-	-
4MS	++++	-	-	tr	-
5MC	++++	tr	-	tr	-
7MD	++++	++	-	-	-
8MD	+++	+++	-	-	-
9MS	++++	+	-	+	-
11MD	++++	+	tr	-	-
12MD	++++	++	-	-	-

Table 3 Average concentrations (in ppm) of trace elements determined by LA-ICP-MS in the epresentativeblack crusts from Dome of Monza.

	Group A				Group B					
	1 MD 16m		4 MS 16m		7 MD 12m		9MS 12m		12 MD 5m	
Element	Average	St.dev	Average	St.dev	Average	St.dev	Average	St.dev	Average	St.dev
As	136	16	151	18	344	28	342	73	302	43
Ba	562	134	308	38	426	13	677	14	4405	109
Cd	13	4	15	6	41	15	223	33	131	56
Cu	118	16	570	168	578	38	548	168	5017	859
Fe	5584	770	36079	9897	69400	8774	84361	43077	255657	3477
Mn	278	27	425	91	907	4	721	268	1956	339
Ni	175	11	53	15	153	5	163	1	258	47
Pb	1464	151	2646	783	18015	2801	18973	3355	34554	1879
Sb	47	8	149	23	559	7	378	145	752	120
Sn	60	14	154	56	436	70	535	257	1033	603
Sr	870	73	1034	61	478	41	1488	796	607	51
V	55	5	118	35	351	33	210	15	550	38
Zn	542	34	462	74	2403	222	1750	430	3632	518

Table 4 Concentration of ions (ppm) in the black crusts collected from the Domeof Monza analyzed with.

		Ion concentrations ppm				
	Sample	**Cl^-**	**NO_2^-**	**NO_3^-**	**SO_4^{2-}**	**Ca^{2+}**
Group A	1 MD	72	0	0	13508	15782
	3 MS	78	222	226	17019	10339
	4 MS	101	47	92	34295	12823
	Average BC	**84**	**90**	**106**	**21607**	**12981**
	St.dev	**9**	**68**	**66**	**6424**	**1573**
Graup B	5 MC	53	0	628	12789	8545
	7 MD	91	201	215	9013	10863
	8 MD	278	35	372	18297	16017
	9 MS	141	45	315	6158	11007
	11 MD	0	42	0	10066	14142
	12 MD	32	69	181	12782	17485
	Average BC	**99**	**65**	**285**	**11518**	**13010**
	St.dev	**45**	**31**	**94**	**1858**	**1535**

Table 5. CC (Carbonate Carbon), EC (Elemental Carbon), OC (Organic Carbon), OX (Oxalate) and TC (Total Carbon) concentrations (wt%) of the collected BCs. Some significant ratios for the analysed BCs are shown. Average values and standard deviations (wt%) were determined for group A and B.

Sample	CC_{TGA}%	EC_{TGA}%	$(EC+CC)_{TGA}$%	OC%	OX_{TGA} %	TC_{CHN} %	OC/EC	EC/TC
1MD	3,32	0,79	4,19	3,25	0,08	7,44	4,09	0,11
3MS	3,52	0,53	4,11	5,73	0,16	9,84	10,81	0,05
4MS	1,48	1,18	2,73	0,69	0,16	3,42	0,58	0,37
Average BC group A	2,77	0,83	3,68	3,22	0,13	6,90	5,16	0,18
St,dev	0,65	0,19	0,47	1,45	0,03	1,87	3,00	0,10
5MC	3,67	0,37	4,09	4,53	0,05	8,62	12,18	0,04
7MD	3,85	1,04	4,93	4,21	0,11	9,14	4,06	0,11
8MD	2,5	2,32	4,93	1,94	0,27	6,87	0,84	0,37
9MS	4,42	1,05	5,73	5,04	0,15	10,77	4,79	0,1
11MD	3,94	0,79	4,88	4,87	0,1	9,75	6,19	0,08
12 MD	3,57	0,53	4,87	4,1	0,17	8,97	3,43	0,13
Average BC group B	3,66	1,02	4,91	4,12	0,14	9,02	5,25	0,14
St,dev	0,26	0,28	0,21	0,46	0,03	0,53	1,15	0,05

Fig. S1. Façade of the Dome of Monza (N Italy) located in the homonymous square.

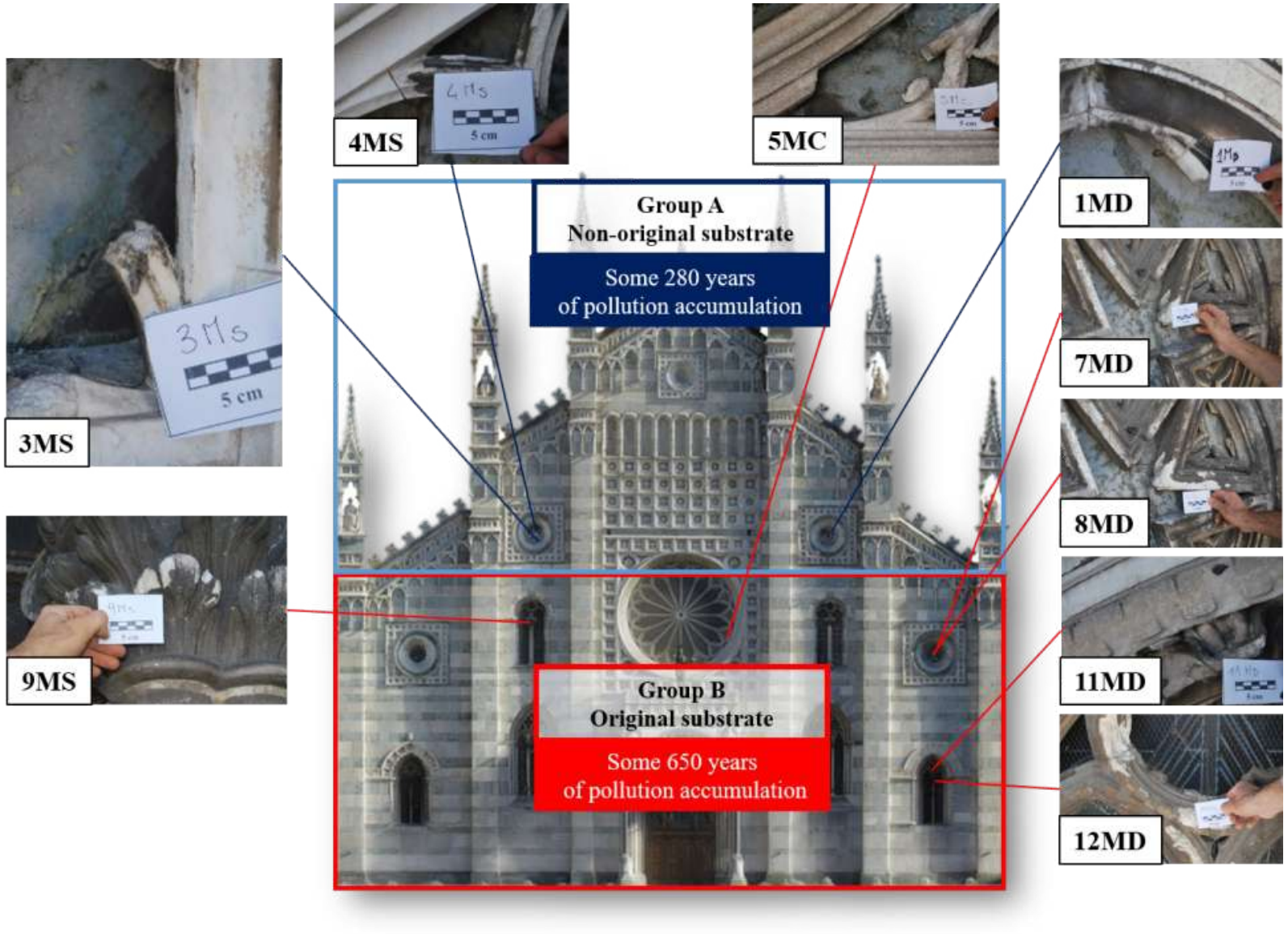

Fig. S2. The locations of sampling points, and photographs of the black crusts collected from the façade of the Dome of Monza.

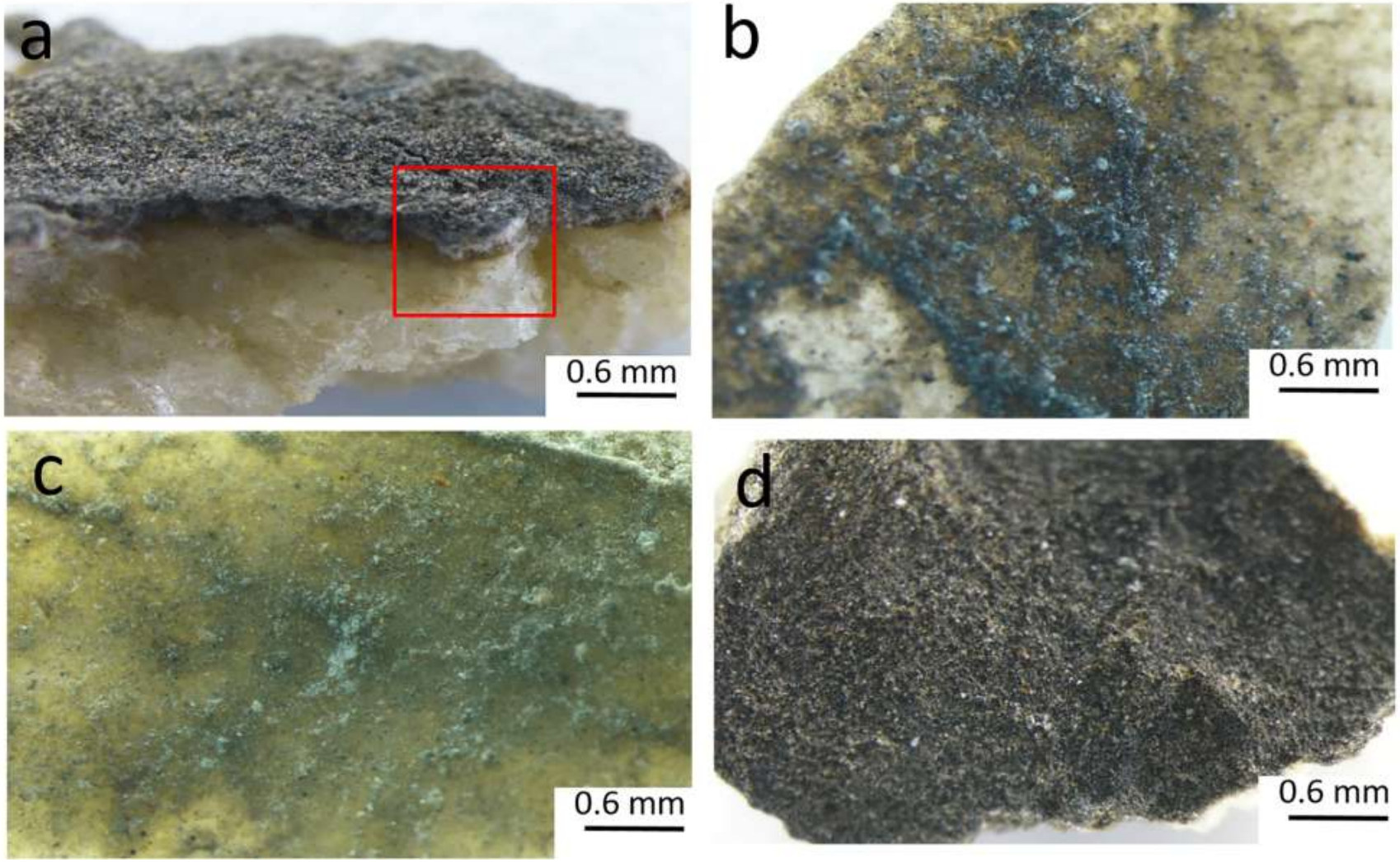

Fig. S3. Stereomicroscope image of black crusts from Monza Cathedral. a and b) 12MD and 11MD samples (5m altitude), c and d) 1MD and 7MD samples (16m and 12 m altitude respectively)..

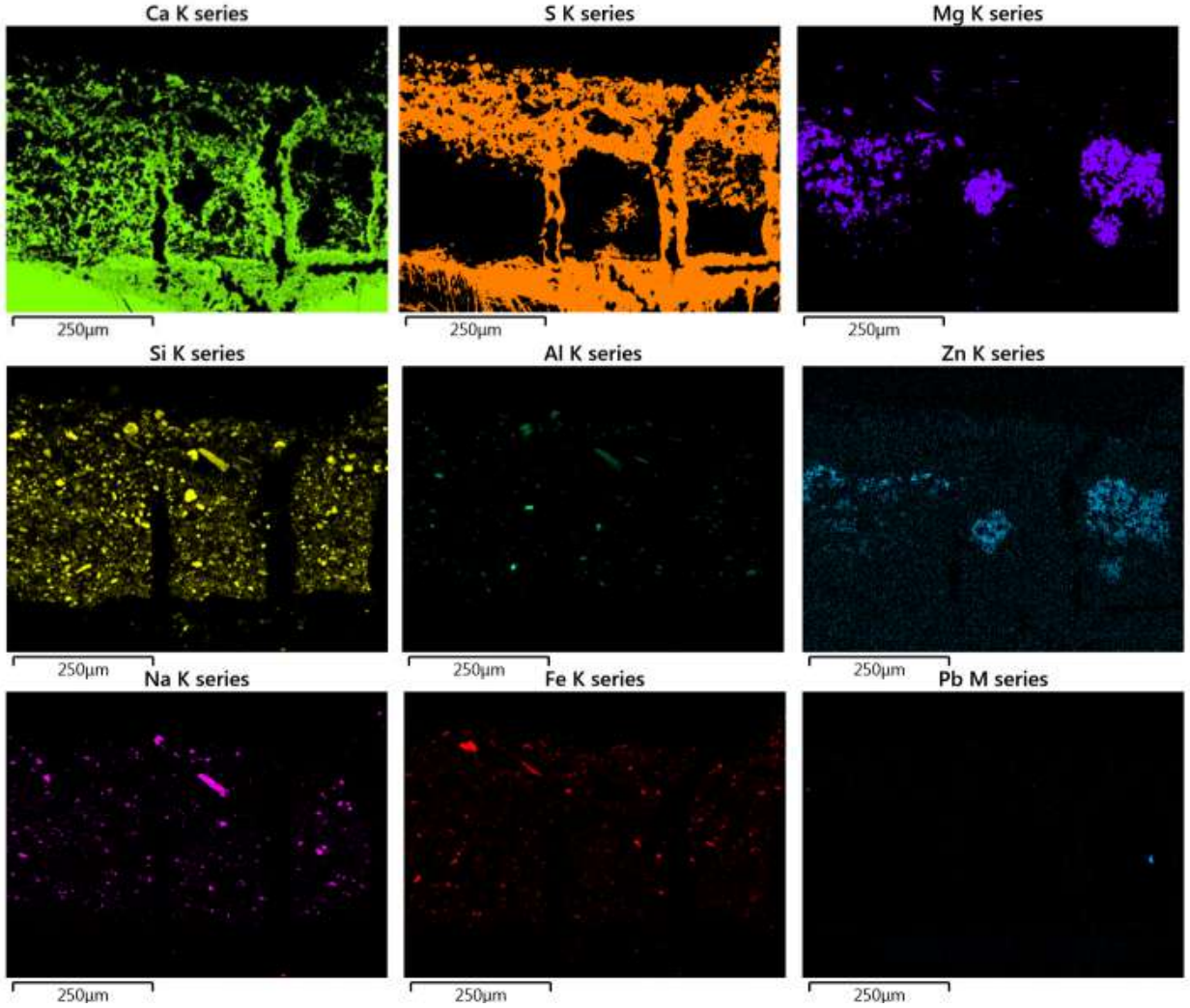

Fig. S4. SEM-EDX elemental mappings of 12MD black crust.

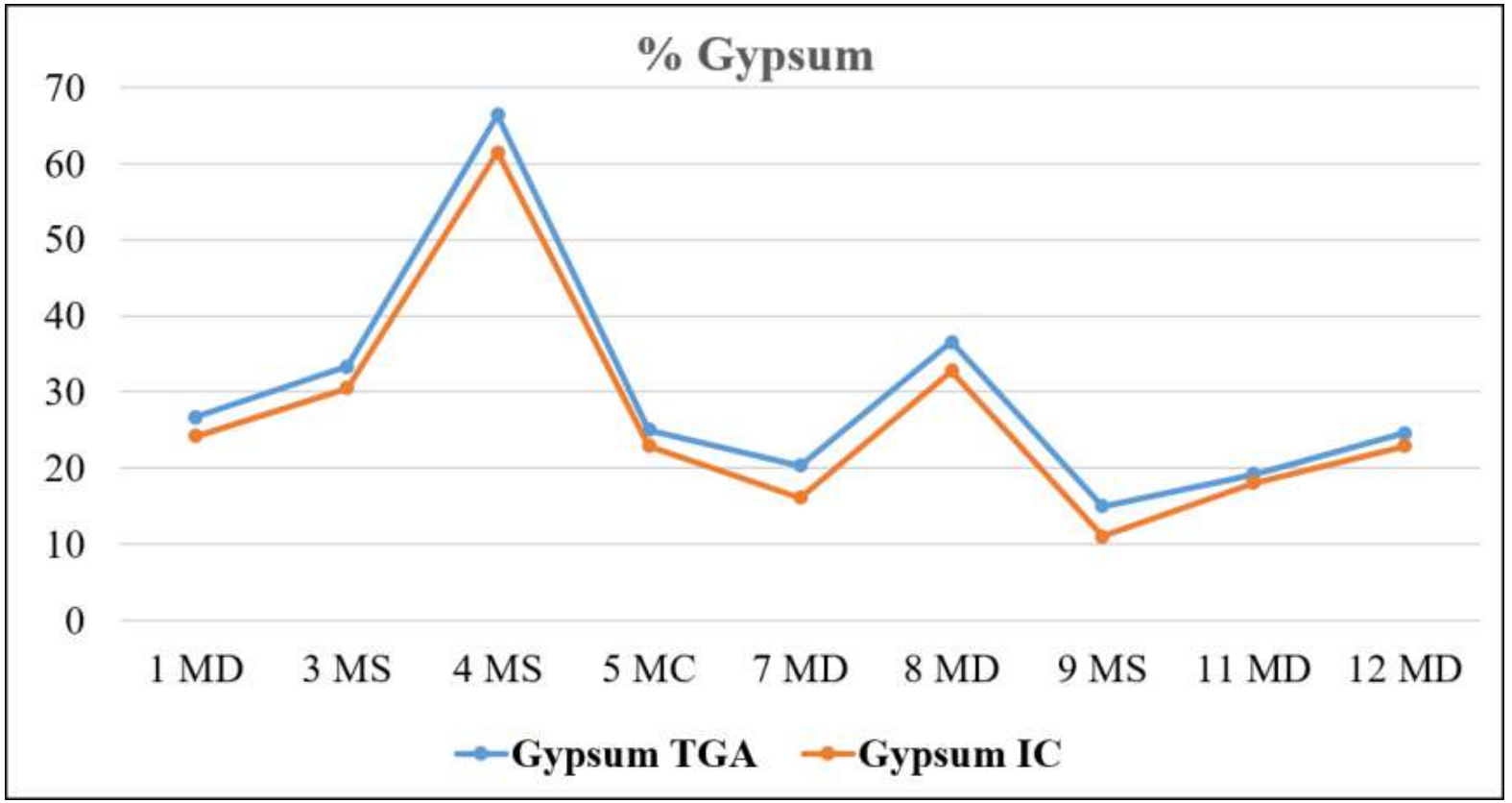

Fig. S5. Percentage of gypsum in the BCs obtained by IC and TGA.